APL Bioengineering REVIEW pubs.aip.org/aip/apb

A review: Blood pressure monitoring based on PPG and circadian rhythm

Cite as: APL Bioeng. 8, 031501 (2024); doi: 10.1063/5.0206980
Submitted: 5 March 2024 · Accepted: 26 June 2024 ·
Published Online: 23 July 2024

Gang Chen,[1] Linglin Zou,[2] and Zhong Ji[1,3,a)]

AFFILIATIONS

[1]College of Bioengineering, Chongqing University, Chongqing 400030, China
[2]Department of oncology, Affiliated Hospital of Southwest Medical University, Luzhou 646000, China
[3]Key Laboratory of Biorheological Science and Technology (Chongqing University), Ministry of Education, Chongqing 400030, China

[a)]Author to whom correspondence should be addressed: jizhong@cqu.edu.cn

ABSTRACT

The demand for ambulatory blood pressure monitoring (ABPM) is increasing due to the global rise in cardiovascular disease patients. However, conventional ABPM methods are discontinuous and can disrupt daily activities and sleep patterns. Photoplethysmography (PPG) is gaining attention from researchers due to its simplicity, portability, affordability, and ease of signal acquisition. This paper critically examines the advancements achieved in the technology of PPG-guided noninvasive blood pressure (BP) monitoring and explores future opportunities. We have performed a literature search using the Web of Science and PubMed search engines, from January 2018 to October 2023, for PPG signal quality assessment (SQA), cuffless BP estimation using single PPG, and associations between circadian rhythm and BP. Based on this foundation, we first examine the impact of PPG signal quality on blood pressure estimation results while focusing on methods for assessing PPG signal quality. Subsequently, the methods documented for estimating cuff-free BP from PPG signals are summarized. Furthermore, the study examines how individual differences affect the accuracy of BP estimation, incorporating the factors that influence arterial blood pressure (ABP) and elucidating the impact of circadian rhythm on blood pressure. Finally, there will be a summary of the study's findings and suggestions for future research directions.

I. INTRODUCTION

According to a report by the World Health Organization (WHO) in 2023, approximately 1.28×10^9 individuals between the ages of 30 and 79 worldwide are affected by hypertension.[1] Shockingly, nearly half of these adults (46%) remain unaware of their condition, while less than half (42%) have received proper diagnosis and treatment.[1] This makes hypertension a leading cause of premature deaths globally. BP provides crucial physiological information related to cardiac function, vascular status, organ perfusion, and hemodynamics. Timely identification of concealed hypertension, nocturnal hypertension, and white coat hypertension is made possible through the utilization of continuous ambulatory blood pressure monitoring (ABPM), thereby enhancing the effectiveness of preventing and treating hypertension.[2] Currently, the conventional method used to periodically measure BP involves inflating and deflating a cuff to impede blood flow. However, this method is unsuitable for early detection and diagnosis of hypertension due to its limitations. Additionally, patient discomfort arises from cuff inflation during use. Invasive arterial cannulation allows for continuous BP measurement, but it is invasive, expensive, and inconvenient to use outside specialized settings, such as operating rooms or intensive care units (ICUs). Noninvasive continuous ABPM has gained more attention compared to clinical invasive methods or traditional intermittent cuff-based measurements.

Due to its cost-effectiveness and convenient extraction, the photoplethysmography (PPG) signal is well suited for continuous monitoring of BP, oxygen saturation, heart rate, respiration, and blood glucose.[3] Consequently, it is widely regarded as the most hopeful noninvasive method for continuously monitoring BP. PPG employs optoelectronic equipment to detect variations in the tissue blood volume without invasive procedures. This method is based on Lambert-Beer's law,[4] which states that light attenuates as it travels through blood due to factors such as path length, tissue density, and absorption. Similar to the intensity of light passing through the skin,[5] periodic fluctuations in the blood volume are observed as blood is ejected from and returned

to the heart. The PPG waveform provides valuable insights into subjects' cardiovascular function and has been theoretically linked to blood pressure regulation.[6]

The waveform of blood pressure and PPG recorded synchronously during dynamic monitoring is depicted in Fig. 1. Their waveform trends exhibit a high degree of consistency, with identical periods observed. Thus, it can be inferred that a robust correlation exists between BP and PPG. The studies conducted by Xing *et al.*[7] and Mousavi *et al.*[8] provide evidence for this correlation.

Consequently, an increasing number of researchers are embarking on investigations into wearable continuous noninvasive blood pressure (CNIBP) monitoring devices based on PPG sensors. To enhance the portability, comfort, and accuracy of these wearables, PPG sensor placement in relevant studies encompasses various locations including fingers,[9,10] wrists,[11,12] upper arms,[13] chest,[14] ears,[15] nose bridge,[16] forehead,[17] and even human epidermis.[18] Moreover, the design of PPG sensors has evolved from single-sensor configurations to multi-sensor integration approaches as well as innovative materials like fiber optic sensors.[10,12,19,20] Currently, integrating PPG sensors into smartwatches represents a promising avenue for development. However, these studies encounter challenges related to noise interference such as motion artifacts that affect the reliability of PPG signals. Furthermore, users have increasingly higher expectations regarding the portability, comfort, and accuracy of wearable devices.

Currently, there are commercially available wearable devices for CNIBP monitoring based on PPG signals. These devices include Somnotouch-NIBP developed by Somnomedic GmbH in Germany,[21] ViSi Mobile System manufactured by Sotera Wireless in the United States,[22] and WATCH D smartwatch designed by HUAWEI in China.[23] Somnotouch-NIBP has obtained CE (Conformité Européenne) certification and enables continuous beat-to-beat BP monitoring. The device comprises a finger PPG sensor and a three-lead electrocardiogram (ECG) connected to an integrated wrist-worn device.[21] After calibrating the device using a cuff placed on the opposite upper arm for BP measurement, pulse transit time (PTT) is derived by measuring the time interval between the R wave on the ECG and the corresponding pulse waveform in the finger PPG signal.[21] The PTT method is used to estimate blood pressure using a nonlinear model. The ViSi Mobile System has received both the United States Food and Drug Administration (FDA) and CE certification, allowing for continuous beat-to-beat monitoring of blood pressure. The system consists of a finger photoelectric plethysmography device and a three-lead ECG. After calibrating with the upper arm cuff on the same side, the pulse arrival time (PAT) is determined by measuring the time delay from the R-peak of the ECG to the position of maximum second derivative in the corresponding PPG waveform.[22] This measurement is then used to estimate BP. WATCH D has received the China National Registration Class II Medical Device Certification. It is equipped with a micro air pump and a bladder cuff, making it compatible with both oscilloscope and PPG technology for BP measurement. Before initiating ABPM, calibration of the BP measurement using the oscilloscope method is necessary. Although these three devices enable wearable CNIBP monitoring, the accuracy of BP estimation diminishes over time, necessitating frequent cuff calibration. The first two devices require chest electrodes for ECG collection, thereby compromising their portability and comfort. Consequently, these three devices still fail to meet users' requirements for accuracy, portability, and comfort in wearable CNIBP monitoring devices, thus becoming a focal point for future research. Table I provides an overview of commercially wearable CNIBP monitoring devices.

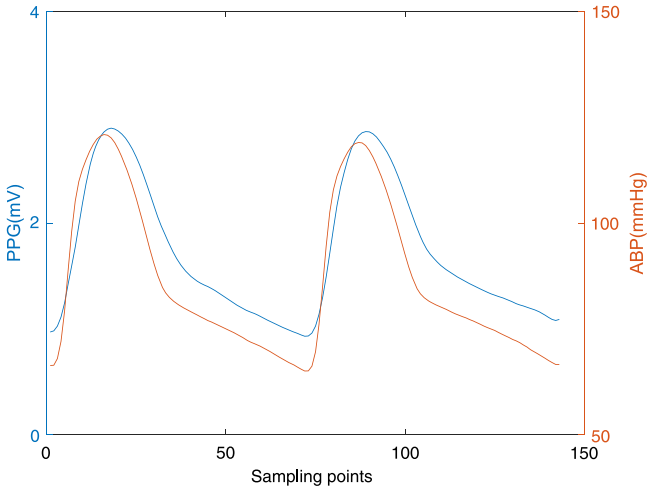

FIG. 1. Comparison of BP and PPG waveforms. The sampling frequency is 125 Hz.

This study presents an overview of the impact of PPG signal quality on the accuracy of BP predictions and recent advancements in cuff-free PPG-based BP estimation. Additionally, it emphasizes the impact of individual variations and circadian rhythms on blood pressure measurements, offering insights for future development of portable continuous ABPM devices utilizing PPG signals. The Web of Science and PubMed databases were searched using keywords such as "Photoplethysmography," "PPG," "blood pressure," "estimation," "signal quality," "quality assessment," "SQA," "SQI," "single PPG," "single Photoplethysmography," "circadian rhythm," "diurnal rhythm," and "day-night rhythm" to find relevant literature. The exclusion criteria were applied as follows:

- Duplicate articles in two search engines
- Patent article
- Review
- Articles unrelated to this study
- Dissertation
- Non SCI articles

According to this exclusion criterion, the screening figures for the second, third, and fourth parts of this study (Figs. 2–4) were obtained.

The article's structure is illustrated in Fig. 5. In step 1, the PPG optical module is employed to collect PPG signals from the finger artery, followed by signal quality evaluation in step 2 (Part II of the article). This section summarizes the impact of PPG signal quality on BP estimation results, encompassing its influence on blood pressure and methods for evaluating signal quality. Subsequently, the PPG input step 3 will be employed for blood pressure estimation by eliminating infeasible signals. Part III of this article elucidates the details of this step, encompassing diverse reported approaches for estimating BP based on PPG signals. These methods include estimation techniques utilizing pulse wave velocity (PWV) or PTT, analysis methodologies grounded in pulse wave analysis (PWA), and estimation methods reliant on individual pulse waves, accompanied by corresponding evaluations. Following that, in step 4, the circadian rhythm of systolic blood

TABLE I. Summary of commercially wearable CNIBP monitoring devices.

Device	Position of PPG sensors	Calibration required	Principles of measurement	Advantages	Disadvantages
Somnotouch-NIBP	Finger-PPG	Initial calibration required	PTT is obtained by synchronously capturing the time interval between the ECG R wave and the corresponding positions of finger PPG waveform. Following initial cuff calibration for BP, PTT is utilized to estimate BP.	Utilizing this technology for beat-to-beat BP estimation, as well as 24-h ECG, pulse oximetry, and actigraphy assessments.	The accuracy of BP monitoring may gradually diminish over time. Not suitable for extended wear due to lack of portability and discomfort.
ViSi mobile system	Finger-PPG	Calibration once per 12 h	ViSi PAT is defined as the temporal delay between the R peak of the ECG and the maximum second derivative of the corresponding PPG waveform. After initial cuff calibration for BP, PAT can be utilized to estimate BP.	By leveraging this technology for beat-to-beat BP estimation, along with continuous assessment of ECG, blood oxygen levels, heart rate, respiratory rate, and body temperature.	The accuracy of BP estimation will gradually decrease over time, so frequent calibration is needed to maintain optimal performance. Not suitable for extended wear due to lack of portability and discomfort.
Watch D	Wrist-PPG	Calibration once per 12 h	BP was measured using an oscilloscope method, employing a micro pump and bladder cuff. Prior to conducting ABPM, calibration was performed by measuring BP with the oscilloscope method, followed by estimation of BP through analysis of wrist PPG waveform.	This portable and comfortable device can be used for ABPM as well as monitoring ECG, heart rate, blood oxygen, and body temperature.	Frequent calibration is necessary to ensure accurate BP estimation.

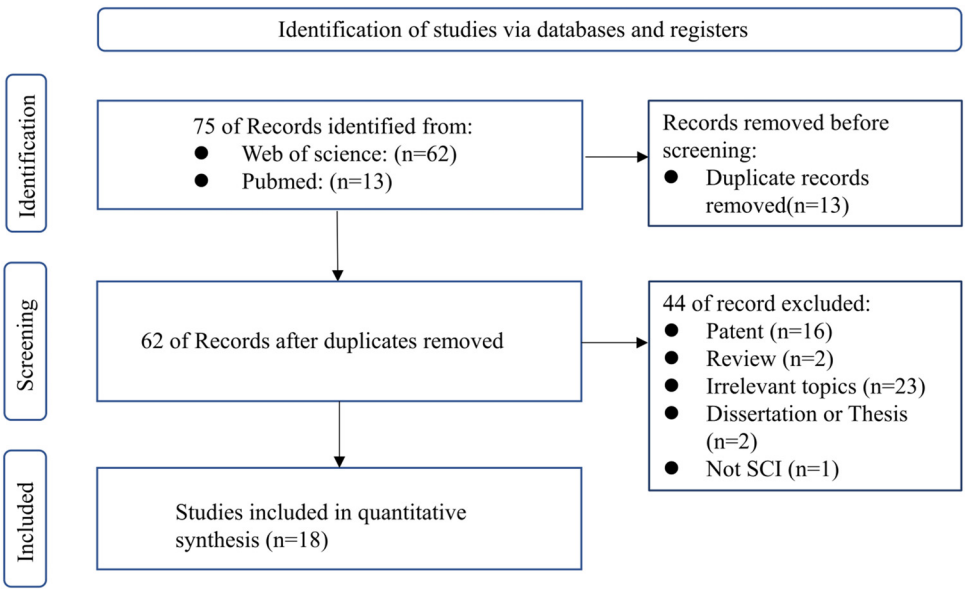

FIG 2. Study flow diagram of signal quality.

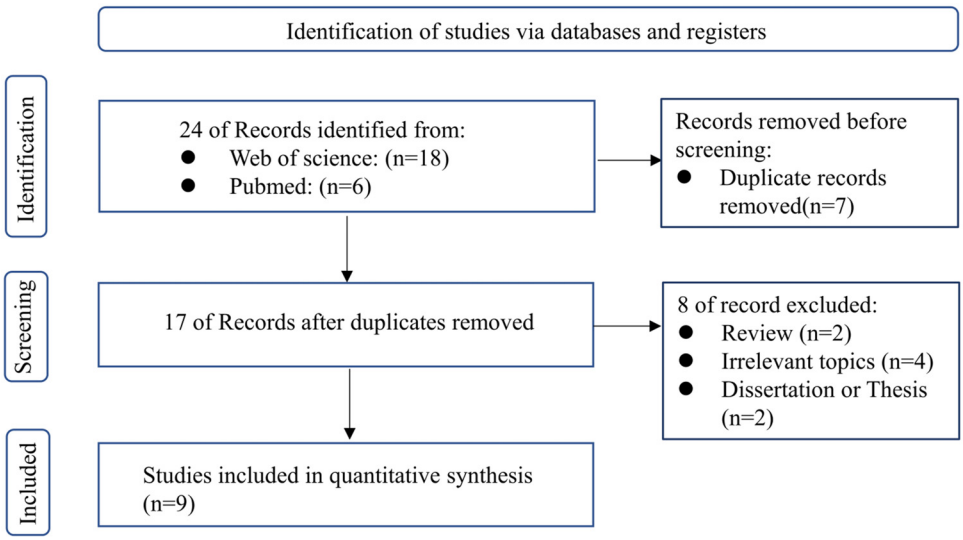

FIG. 3. Study flow diagram of blood pressure estimate.

pressure (SBP)projected from step 3 will be utilized to self-correct the blood pressure prediction model from step 3, thereby ensuring accuracy and stability in continuous blood pressure prediction. In Part IV of this article, we discussed the influence of individual differences on the accuracy of blood pressure estimation, encompassing factors impacting ambulatory blood pressure and the circadian rhythm's effect on blood pressure. Finally, continuous blood pressure values estimated based on PPG and circadian rhythm guide long-term monitoring of subjects from step 4 back to step 1. Section V offers a detailed discussion along with potential directions for future research. At the conclusion of the article, Part VI presents a comprehensive overview of the entire study.

II. EFFECT OF PPG SIGNAL QUALITY ON BLOOD PRESSURE ESTIMATION RESULTS

A. Effect of noise in PPG signals on blood pressure estimation results

The accurate recognition of signal features in PPG signals is compromised due to their inherent nonlinearity and non-stationarity, as well as their susceptibility to various forms of noise.[24] This adversely affects the precision and stability of models used for BP prediction. Particularly, the presence of arm or finger movements can introduce motion artifacts that may alter PPG waveforms, rendering them unsuitable for diagnostic purpose and potentially leading to significant

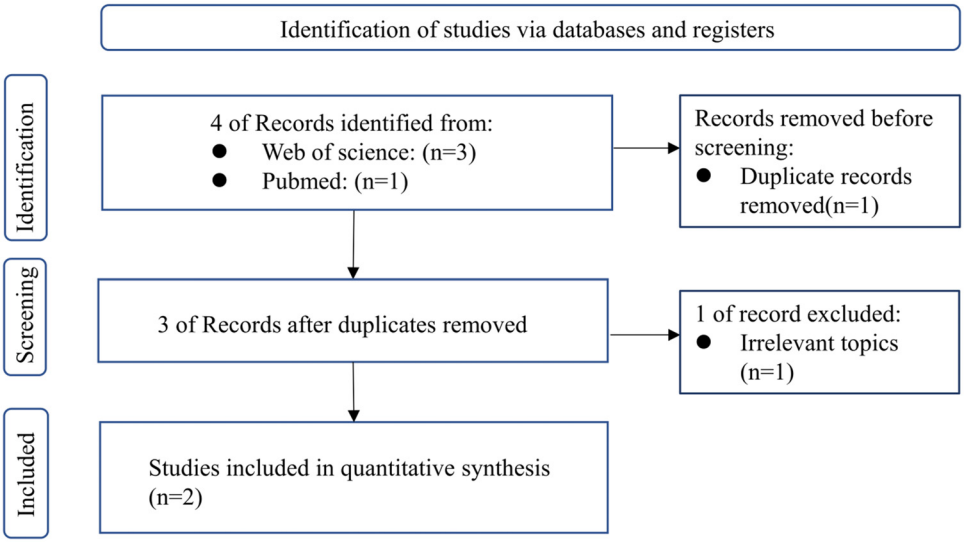

FIG. 4. Study flow diagram of individual difference.

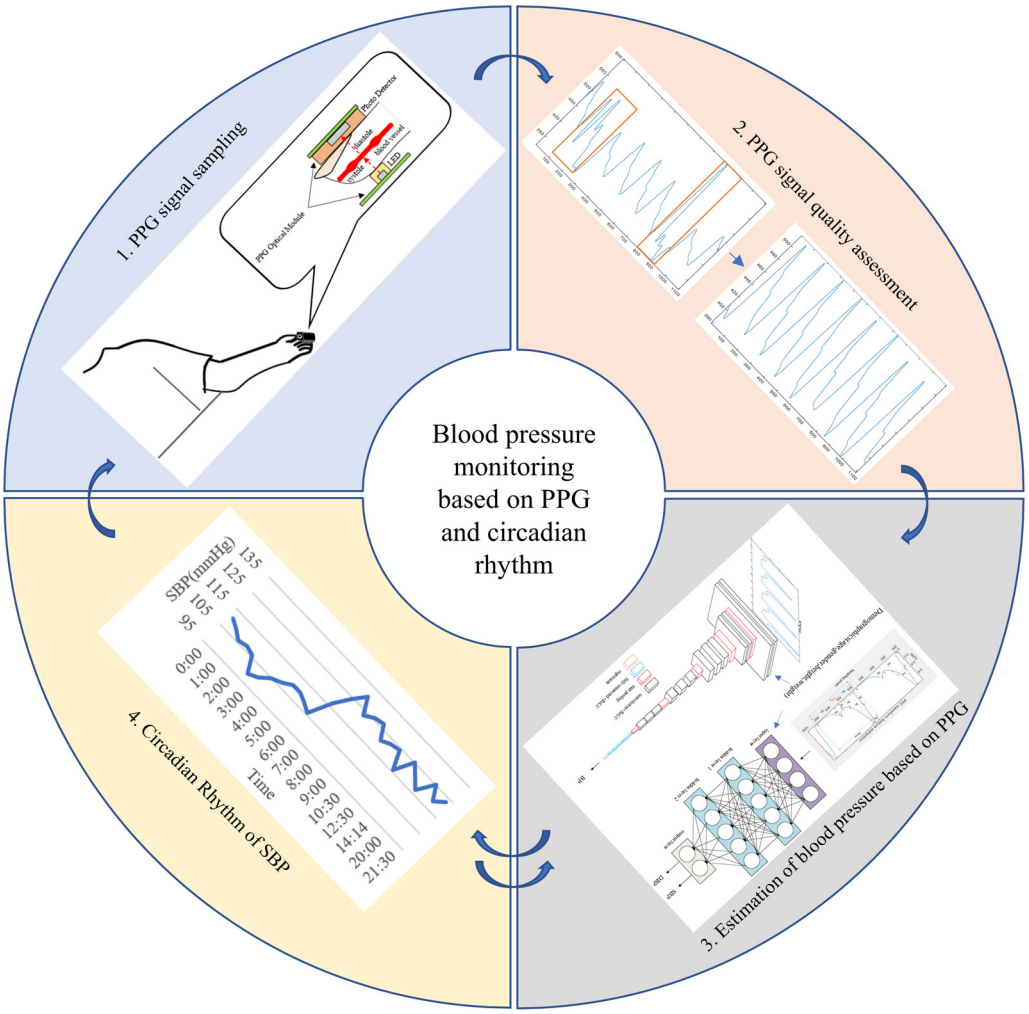

FIG. 5. Article's structure figure.

medical problems.[25] Hence, noise reduction plays a pivotal role in signal research.[26] For PPG signals, which have a primary frequency band ranging from 0.5 Hz to 5 Hz, linear filters prove effective in denoising when there is minimal overlap between their spectrum and that of the noise.[27,28] However, when the noise exhibits a wide spectrum characteristic, resulting in aliasing of both the signal and noise spectra, conventional filtering methods may induce signal distortion.

The generation of noise in the PPG signal is primarily attributed to physiological factors, such as exercise or muscle contraction, and non-physiological factors, including signal loss caused by continuous electrical stimulation, device displacement, or network disconnection.[28–31] Furthermore, various other factors can also impact the PPG waveform, encompassing respiration, low blood flow perfusion, temperature at the measurement site, skin pigmentation, alignment of light source and photodetector, sensor-skin connection quality, contact pressure level applied during measurement process as well as subject posture and ambient light conditions.[32–37] These sources of interference compromise the integrity of the PPG signal and subsequently influence blood pressure monitoring outcomes. Henceforth, it becomes imperative to promptly identify and eliminate invalid signals for subsequent signal analysis.

B. Methods for determining the performance of PPG signals

Currently, methods for evaluating the usability of PPG signals can be broadly categorized into three groups: PPG waveform feature-based approaches, template matching techniques, and machine learning (ML)/deep learning (DL) methods.[38,39] The signal quality evaluation, utilizing the three methodologies, is succinctly outlined in Tables II and III as provided herein. Among these methods, the first two belong to traditional approaches that initially extract various signal quality indexes (SQIs) from PPG signals and subsequently classify pulse waves into either clean or damaged categories or further divide them into clean, acceptable, and damaged categories based on heuristic rules, empirical judgment, or thresholds determined by ML

TABLE II. Summary of signal quality assessment based on the PPG waveform feature method.

Category	Study	Dataset	Samples	Classification grade	Result
PPG waveform features	42	Guilin People's Hospital' data	219	3	The final evidence demonstrates that the fourth-order Chebyshev II filter exhibits superior efficacy in enhancing the SQI of PPG.
	49	MIT-BIH/ BIDMC	16/53	2	ECG MAPE 3.9%, 3.6%, PPG MAPE 6.0%, BP MAPE 5.0%
	50	MAHNOB-HCI/Vicar	–/10	···	The sensitivity and accuracy of peak detection were 97.35% and 98.25%, 97.83% and 97.02, respectively.
	44	MIMIC II/III	···	2	The outliers could be efficiently filter out.
	45	MIMIC II, CONTEC, E4, Capnobase	···	···	The algorithm suggested has demonstrated remarkably better results in the context of wearables, with an F_{score} surpassing 0.92.
	46	MIMIC II/III	150	2	SBP SD 3.24 mmHg MAE 2.38 mmHg, DBP SD 1.73 mmHg MAE 1.23 mmHg. Compared to not using SQA, the accuracy of SBP and DBP increased by 19.56% and 24.61%, respectively.
	47	MIMIC II	12 000	2	The SD of prediction errors for SBP and DBP increased by 11.68% and 10.81%, respectively. The MAE increased by 14.79% and 11.70%, respectively
	48	Volunteers' data/MIMIC III/CSL	471/16199/605	3	The RF classifier demonstrated superior performance with an overall mean accuracy of 96.8%. Other evaluation indicators in the confusion matrix all exceeded or approached the threshold of 0.98.
	43	Volunteers' data	20	2	During exercise, the MAE of SBP and DBP decreased from 36.6 and 13.6 mmHg to 4.8 and 3.47 mmHg
	41	MIMIC III	···	2	F1:97%
	52	Volunteers' data	8	2	The balance accuracy (BACC) of green light, red light, and infra-red light increased by 21.3%, 21.6%, and 19.0%, respectively.

algorithms. Currently available SQI extraction methods primarily rely on statistical principles, time domain analysis techniques, frequency domain analysis methods as well as template matching techniques.[40]

1. PPG waveform feature method

The PPG waveform feature methods typically involve the derivation of temporal, spectral, or pattern-related features from an individual pulse wave. These extracted features are subsequently utilized for classification purpose based on a predetermined threshold. Elgendi *et al.*[41] conducted an evaluation and comparison of eight SQIs extracted from PPG. They discovered that skewness (S_{SQI}) emerged as the most suitable indicator for assessing PPG signals, offering potential applications in enhancing the diagnosis and monitoring of abnormal BP conditions. According to the research findings of Elgendi *et al.*,[41] Liang *et al.*[42] aimed to determine the optimal filter type and sequence

TABLE III. Summary of signal quality assessment based on the template matching method and ML/DL methods.

Category	Study	Dataset	Samples	Classification grade	Result
Template matching	54	Volunteers' data/MIMIC II	19/–	2	Volunteers' data: accuracy: 91.5% ± 2.9%, sensitivity: 94.1% ± 2.7%, specificity: 89.7% ± 5.1%. MIMIC II: accuracy: 98.0%, sensitivity: 99.0%, specificity: 96.1%.
ML/DL	60	Volunteers' data	10	3	The sensitivity and specificity of high-SQI PPG are 0.81 and 0.9, while the sensitivity and specificity of low-SQI PPG are 0.84 and 0.93.
	61	Volunteers' data	76	2	balanced accuracy: 0.975, Sensitivity: 0.964, specificity:0.987
	62	MESA	2055	2	···
	63	MIMIC II	12 000	2	The proposed probabilistic filtering framework significantly enhances the accuracy of BP estimation compared to using raw data.

configuration for effectively reducing noise and enhancing signal quality in both original and filtered PPG signals. Initially, the signal segments were classified into three categories (G1: excellent, G2: acceptable, and G3: unqualified) using S_{SQI}. Subsequently, various types of filters were employed for signal filtering, with S_{SQI} used to evaluate the effectiveness of these filters. The results indicated a significant improvement in the SQI when employing a fourth order Chebyshev II filter. Hayashi *et al.*[43] employed support vector machines (SVM) as a classifier to categorize PPG signals into acceptable and unqualified signals across various conditions, including rest, exercise, and recovery. They utilized the S_{SQI} feature to eliminate low-quality signals, with the aim of enhancing diagnostic accuracy and healthcare standards. Following the removal of unqualified signals using S_{SQI}, both SBP and diastolic blood pressure (DBP) predicted mean absolute errors (MAE) notably decreased, particularly during exercise state where SBP reduced from 36.6 mm Hg to 4.8 mm Hg and DBP decreased from 13.6 mm Hg to 3.47 mm Hg. The noise elimination technique proposed by Lin *et al.*[44] relies on the analysis of pulse wave characteristics to effectively filter out outliers. Five evaluation indicators were initially extracted from the pulse wave. Median filtering was then used to derive median lines corresponding to these indicators. An acceptable threshold range was established near each median line for individual pulse evaluation. If any feature value exceeds the predetermined threshold, the corresponding part of the pulse is eliminated. A new method proposed by Banerjee *et al.*[45] uses frequency domain analysis to evaluate the quality of PPG signals. Metrics for assessing signal quality were derived from the spectrum's cardiac and respiratory components, while a differential evolutionary algorithm was employed to optimize threshold. Roy *et al.*[46] utilized four features, namely, approximate entropy, spectral entropy, Hjorth complexity, and Higuchi fractal dimension, as input feature vectors for the self-organizing map binary classifier to distinguish between "clean" and "damaged" classes. The evaluation was conducted using over 150 samples from the MIMIC II/III waveform database. Compared to not utilizing signal quality assessment (SQA), the accuracies of SBP and DBP improved by 19.56% and 24.61%, respectively. Salah *et al.*[47] proposed a continuous two-step cleaning technique, which consists of an initial mild threshold screening to identify clearly abnormal signals, followed by a fine cleaning using the principal component analysis (PCA). The model's performance was enhanced when trained on the processed data, leading to a reduction in the prediction error and an increase in the correlation between predicted and actual blood pressure values. Prasun *et al.*[48] employed a combination of time and frequency domain analysis to derive seven distinct features, which were then integrated and applied with various ML classifiers for the purpose of classifying signals into three categories (clean, partially clean, and damaged). The final random forest (RF) classifier demonstrated extraordinary performance, achieving a mean accuracy of 96.8% in evaluations across four datasets. The other evaluation indicators in the confusion matrix exceed or approach the threshold of 0.98.

Furthermore, novel measurement methods based on PPG waveforms have been proposed by researchers. Adami *et al.*[49] proposed a universal framework that employs the techniques of empirical mode decomposition and discrete wavelet transform for simultaneous decomposition of electrocardiogram (ECG), PPG, and BP signals. This decomposition process generates respiratory signals such as ECG-derived respiration (EDR), PPG-derived respiration (PDR), or BP-derived respiration (BDR). Subsequently, the signal purity index (SPI) is computed for each respiratory signal at different time points, serving as the SQI to assess signal quality based on the Hjorth parameter. Additionally, an evaluation of signal quality parameters is performed in conjunction with the extended Kalman filter to mitigate the impact of low-quality segments during estimation. Furthermore, EDRs, PDRs, or BDRs are fused together to estimate respiratory rate. Experimental evaluations were conducted using both MIT-BIH multi-channel sleep map database and Beth Israel Deaconess Medical Center (BIDMC) database yielding mean absolute percentage errors (MAPE) of 3.9% and 3.6% for ECG signals, respectively, while MAPE values for PPG and BP signals were found to be 6.0% and 5.0% correspondingly. Based on the spectral characteristics of remote photoplethysmography (rPPG), Fan *et al.*[50] proposed a metric to assess signal quality for accurate estimation of PTT. This metric aims to identify high-quality signals, detect any potential noise, and assess the overall reliability of rPPG measurements. The sensitivity and accuracy of peak detection evaluated using the MAHNOB-HCI dataset and Vicar dataset were 97.35% and 98.25%, respectively, as well as 97.83% and 97.02%. Schmith *et al.*[51] conducted a comprehensive quality evaluation of PPG signals by analyzing the shape of short segmented attractors in an analytical manner. This approach demonstrated effective classification performance for both good and bad PPG signal segments, F1 score achieved 97%. Although slightly inferior to DL methods in terms of results, this completely analytical method eliminated the need for training or calibration, rendering it highly suitable for real-time applications. The PPG quality metric proposed by Tiwari *et al.*[52] is based on modulation spectrum characteristics. Experimental results on multi-wavelength PPG datasets demonstrated that the combination of the proposed metric and traditional metrics outperformed several conventional SQIs significantly. Specifically, the balance accuracy (BACC) for green, red, and infrared light was improved by 21.3%, 21.6%, and 19.0%, respectively.

2. Template matching method

The template matching method is a commonly employed technique for assessing regularity in PPG signal segment classification, as high-quality signal segments are expected to exhibit similar pulse wave shapes.[53] Lim *et al.*[54] utilized principal component analysis to generate multiple primary templates and subsequently updated these templates based on the incoming clean PPG pulses. Correlation coefficients were then employed to classify PPG pulses into two categories: good and bad. In comparison with volunteer data, this algorithm exhibits superior accuracy, sensitivity, and specificity on the MIMIC II database. The signal quality evaluation method developed by Papini *et al.*[55] involves the utilization of dynamic time warping barycenter averaging of multiple pulses, based on a template approach. Notably, this method exhibits enhanced stability in performance as it eliminates the need for alignment processes within the set. Song *et al.*[56] proposed an adaptive matching template algorithm based on rules to evaluate the quality of PPG waveforms. This algorithm computes the correlation coefficient between an individual PPG waveform and a mean template of PPG waveforms. The primary focus of this approach is to judge signal quality by analyzing variations in both signal amplitude and time difference. However, due to its limited adaptability, researchers have begun exploring alternative solutions that leverage the morphological characteristics of PPG signals. Alam *et al.*[57] utilized a combination of template matching and kurtosis to classify the quality of PPG signals.

The accuracy of classifying 96 500 signal segments was 96.5%. The initial application of the incremental-merge segmentation algorithm by Yang *et al.*[58] involved the identification of the peak and onset of the PPG signal beat, followed by a combination of thresholding and adaptive template matching to evaluate the quality classification of the PPG signal. Gazi *et al.*[59] employed two template matching techniques along with two distinct thresholds to effectively eliminate outliers present in PPG signal beats.

Traditional template matching and PPG waveform feature methods often exhibit limited accuracy and database-specific overfitting, thereby constraining their universality.

3. Machine learning/deep learning methods

With advancements in computer science and technology, an increasing number of researchers are utilizing ML/DL methods to evaluate the quality of PPG signals. In a study conducted by Liu *et al.*,[60] a fuzzy neural network with five-layer was utilized to assess the SQI. Based on the observed changes in the output of each stroke measured using commercial equipment, the signals quality are classified into three categories. By calculating the stroke output from PPG and inputting extracted parameters into their developed model, they assessed the performance of SQI evaluation. The research findings demonstrate that PPG with high SQI and low SQI exhibit comparable levels of sensitivity and specificity. Roh *et al.*[61] utilized a convolutional neural network (CNN) to transform PPG signals into 2D images and successfully classified them into two distinct categories. The resulting model demonstrated notable sensitivity and specificity. Rinkevičius *et al.*[62] proposed an algorithm that utilizes ECG guidance to assess the quality of PPG signals. The algorithm accurately identifies the onset of the PPG pulse by detecting R and T waves in the ECG signal. Subsequently, it calculates the absolute second derivative of the PPG signal envelope and applies thresholds to identify lower-quality PPG pulse waves. Chen *et al.*[63] proposed a data-driven model that utilized the maximum entropy principle to select a probability model for evaluating beat-to-beat quality of PPG signals, followed by signal filtering based on physiological rules.

Despite the commendable performance of ML/DL in evaluating PPG signal quality, certain challenges persist. These include the presence of multiple model parameters, prolonged computation time, and the need for a significant amount of annotated data to aid in model training and validation. The laborious task of manually annotating thousands of PPG signals by experts further restricts the suitability of such methods primarily to offline applications.

III. THE PPG-BASED METHOD FOR BLOOD PRESSURE EVALUATION

A. The PWV or PTT methods for assessing blood pressure

PWV or PTT is a widely used indicator for estimating BP. PTT is a metric that measures the time difference between pulse waves in different segments of the arterial system. It has an inverse correlation with PWV. Additionally, the PAT can be determined by calculating the time between the R peak on an ECG and the peak in PPG. There are two common methods for measuring PTT/PAT. The first involves synchronously acquiring ECG and PPG signals. The second involves using multiple sensors placed at both extremities to calculate temporal intervals between signals from different anatomical regions.

PWV is primarily influenced by arterial vascular compliance. The M-K equation (1) was derived in previous studies by considering the propagation of pulse waves and the correlation between vascular parameters and pulse wave velocity. This equation was first introduced by Moens and Korteweg,[64,65]

$$\mathrm{PWV} = \sqrt{\frac{Eh}{\rho D}}. \tag{1}$$

Among them, E represents the arterial elastic modulus, h refers to the thickness of the arterial wall, D signifies the inner diameter of arterial, and ρ stands for the blood density. After calculating PTT/PWV/PAT, the mentioned equation can be utilized to estimate BP. The study conducted by Lazazzera *et al.*[66] involved strategically placing two sensors on the front and back of the smartwatch to simultaneously capture PPG signals from both the wrist and fingertips. By incorporating time intervals of PPG readings from these two locations into a linear model, they successfully achieved accurate estimation of blood pressure. The accuracy assessment was performed on a sample size consisting of 44 participants, yielding results that closely aligned with the standards set by AAMI. Tabei *et al.*[67] used mobile phone cameras to simultaneously capture PPG signals from both index fingers, which were then utilized for estimating BP by calculating PTT.

Furthermore, PPG is integrated with other physiological signals to estimate blood pressure by determining the spatial separation between two anatomical points and calculating PTT or PAT. Marzorati *et al.*[68] successfully estimated blood pressure by combining PPG with phonocardiogram (PCG) to continuously extract PAT. Huynh *et al.*[69] combined impedance plethysmography (IPG) sensors with PPG sensors placed on the wrist and index finger, respectively, to calculate PTT and estimate BP. Yousefian *et al.*[70] utilized ballistocardiography (BCG) and PPG signals collected from a wristband to estimate BP. They employed wrist PTT as proximal and distal timing benchmarks for BCG data analysis. Table IV presents an overview of the PTT methods utilized in this article for assessing BP.

The BP assessment methods mentioned above, which are based on PWV or PTT, require the use of at least two sensors, resulting in increased cost and noise as well as challenges to portability. Furthermore, owing to interindividual physiological variations, these methods exhibit suboptimal accuracy in estimation and require frequent calibration.

TABLE IV. Summary of the PTT methods for assessing blood pressure.

Study	Signals acquisition method	Subjects	Result (mmHg)	
			SBP	DBP
66	Wrist PPG + finger PPG	5 + 44	ME: −1.52 STD: 9.45	ME: 0.39 STD: 4.93
67	Both index finger PPG	6	MAE: 2.07 STD: 2.06	MAE: 2.12 STD: 1.85
68	Finger PPG + Chest PCG	20	MAE: 3.06	MAE: 1.83
69	Finger PPG + Wrist IPG	15	RMSE: 8.47 STD: 0.91	RMSE: 5.02 STD: 0.73
70	Wrist PPG + Wrist BCG	22	MAE: 7.6	MAE: 5.1

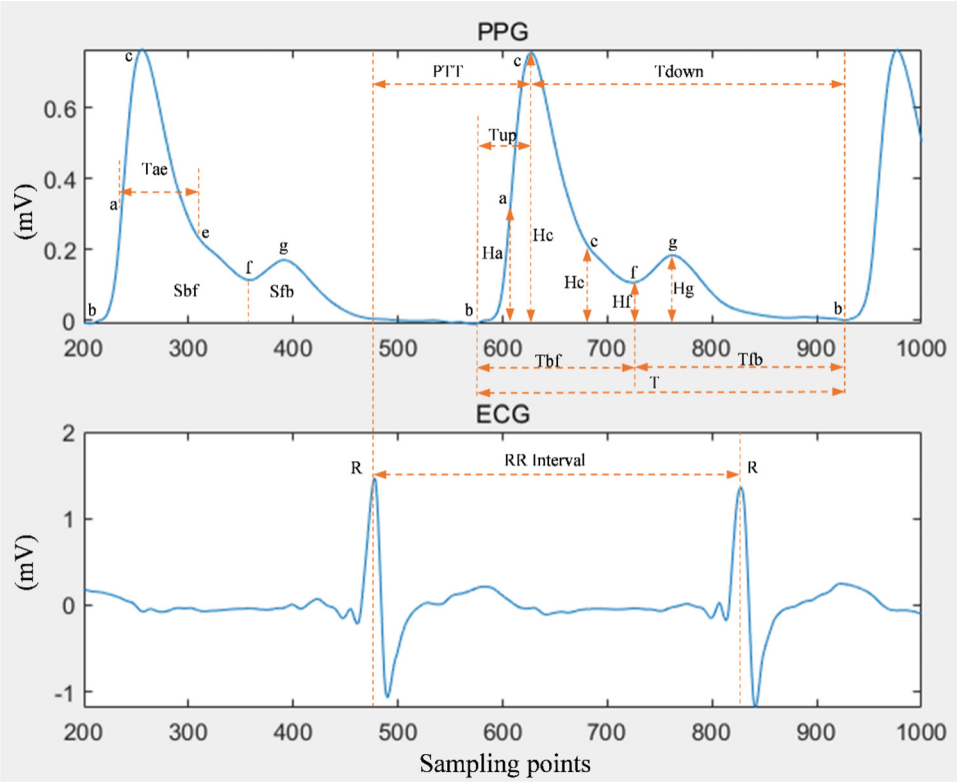

FIG. 6. Partial PPG feature schematic diagram. The sampling frequency is 500 Hz.

B. The PWA method for assessing blood pressure

The data collected from the PPG waveforms included various physiological information. They also exhibited strong correlations with the cardiovascular system. Confirming the physiological meaning of pulse waves, PWA extracts comprehensive features from PPG and associated waveforms using robust artificial intelligence algorithms to estimate BP. The investigation into techniques for predicting BP using PWV can currently be categorized into two primary domains: exploring features that demonstrate a robust connection with BP and enhancing artificial intelligence algorithms through optimization methods. The association between BP and several characteristics of the PPG waveform, including the aforementioned PTT, has been experimentally validated. The features utilized in previous studies can be categorized into characteristics in the temporal domain, characteristics in the frequency domain, demographic data, and so forth. Specific details regarding these features are illustrated in Fig. 6.

ML technology is used to explore the nonlinear relationship between the PPG signal and BP, resulting in a breakthrough for BP prediction models. Chen *et al.*[71] utilized an open dataset to extract 14 characteristics from both ECG and PPG signals, carefully selecting these characteristics based on the mean impact value (MIV) index. Subsequently, a genetic algorithm was employed to optimize a support vector regression (SVR) model for precise BP prediction. Tan *et al.*[72] conducted a study in which they simultaneously captured PPGs and ECGs from 10 subjects and screened time-domain features using the MIV index. This study used a BP network with genetic algorithms (GA) to build models for SBP and DBP. The proposed algorithm demonstrated superior performance compared to both traditional regression models and ANN. However, it is important to note that the credibility and generalizability of the model may have been affected by the limited number of subjects used in the above-mentioned two studies.

Furthermore, several studies have utilized more intricate DL models to estimate BP by extracting pertinent PPG features. Li *et al.*[73] used the DL framework to estimate BP by extracting seven features, including PTT. The DL framework comprises bidirectional temporal layer and multilayer long short-term memory (LSTM) incorporating a residual blocks. Evaluation using the MIMIC II dataset demonstrated that the estimated SBP achieved grade B accuracy according to the BHS standard, while DBP attained grade A accuracy. Senturk *et al.*[74] assessed the accuracy of three ML models for estimating BP by extracting features from the MIMIC II data and combining them with some chaotic features. The research demonstrated that nonlinear autoregressive neural networks with external inputs (NARX) outperformed other models. However, the size of the dataset used is not explicitly stated, which could impede comparisons of results between studies. In this article, Table V presents the method used for estimating BP using through PWA.

The method used to estimate BP through PWA involves a multitude of extracted feature parameters, and the screening process for determining these parameters is intricate, resulting in significant disparities in estimation outcomes. Furthermore, due to the potential

TABLE V. Summary of the PWA methods for assessing blood pressure.

Study	Dataset	Features	Algorithm	Result (mmHg)	
				SBP	DBP
71	MIMIC III	14	GA-SVR	MAE: 3.27 STD: 5.52	MAE: 1.16 STD: 1.97
72	Volunteers' data 10 subjects	17	GA-BP	RMSE: 2.114	RMSE: 1.3
73	MIMIC 50 subjects	7	BiLSTM + residual-LSTM	MAE: 6.726 STD: 14.505	MAE: 2.516 STD: 6.442
74	MIMIC II	19	NARX-NN	MAE: 0.0224 STD: 2.211	MAE: 0.0417 STD: 1.2193

inclusion of irrelevant features and inadequate exploration of information embedded within PPG waveforms, the accuracy of PPG waveform benchmark detection becomes crucial in determining the results.

C. The method of using single PPG to assess blood pressure

Currently, technology based on PTT and PWA can achieve acceptable accuracy for cuff-free blood pressure measurement. However, these methods require multiple sensors, such as PPG and ECG, to collect physiological signals. This limits their suitability for truly wearable applications. Therefore, Khalid *et al.*[75] compared the accuracy of three ML algorithms in assessing BP. The algorithms utilized only three essential pulse features extracted from high-quality PPG signals: area, rise time, and 25% pulse width. The results demonstrated that the regression tree (RT) performed the best. Furthermore, they also evaluated the estimation accuracy for three different clinical blood pressure categories: normal blood pressure, hypertension, and hypotension. A noninvasive and continuous method for assessing BP using a single PPG sensor was proposed by Hu *et al.*[76] They considered the formation mechanism of PPG signals and employed a three Gaussian model to extract features. XgBoost was identified as the optimal model for BP estimation. Dey *et al.*[77] developed a model for BP assessment using lasso regression, which incorporated demographic information and PPG features. The threshold for dataset classification was determined by using the median value of demographic information. The demographic information from different categories was combined with PPG features and inputted into their respective prediction models to estimate blood pressure. Acciaroli *et al.*[78] conducted a dynamic system analysis to estimate BP from PPG signals using an autoregressive exogenous (ARX) model based on kernel regularization. The feasibility of this approach was assessed by analyzing PPG time series obtained from multiple individuals in 10 resting states. The results demonstrate that the method achieved an average root mean square error (RMSE) of 6.5 mm Hg over a short duration. However, it is important to note that the data used for model training and validation in this method are sourced from the same participant, which can result in overfitting issues.

Recent rapid advances in DL have enabled numerous research efforts to extract complex multidimensional features from PPG signals and apply advanced convolutional processing capabilities to continuous BP monitoring. Baek *et al.*[79] proposed an integrated CNN model for predicting BP without the need for feature extraction. They also explored the combination of PPG signals with different wavelengths using this approach. The results showed that green PPG provided better BP prediction performance for most subjects, achieving similar accuracy as other methods using single PPG. Sadrawi *et al.*[80] proposed a genetic algorithm-optimized deep convolutional autoencoder to explore the potential of using a single PPG signal for generating successive arterial blood pressure (ABP). Ma *et al.*[81] introduced KD-transformer, a method based on transformer architecture that incorporates a knowledge distillation strategy for accurately estimating BP waveforms. To extract informative features from PPG signals while accounting for inherent physiological parameter variations and noise, this approach employs a strategy of backtracking feature reduction and feature combination. To mitigate motion artifacts, Pankaj *et al.*[82] proposed a DL framework for estimating BP. The framework utilizes a single-channel PPG signal through superwavelet transform and optimization while simultaneously classifying the BP. The superwavelet transform method is used to convert 1D PPG signals into 2D super-resolution spectrograms. This approach effectively separates the true components of the PPG signal from peak values associated with motion artifacts, thereby achieving artifact removal. Establishing a benchmark is crucial for evaluating the increasing number of ML methods that utilize PPG signals for BP estimation. González *et al.*[83] extensively compared 11 state-of-the-art models on four different datasets, across feature-to-label, signal-to-label, and signal-to-signal categories. They employed mean absolute scaled error (MASE) as an evaluation metric for comparing BP models across various datasets. Table VI presents the methods discussed in this article for estimating BP using a single PPG.

The ML methods mentioned above are mainly used for single-point or short-term blood pressure measurement, which does not meet the clinical needs of continuous long-term blood pressure monitoring. However, the use of DL approaches fails to meet the interpretability requirements of feature parameters and estimation models in the medical field due to their algorithmic black box nature. Additionally, DL models have numerous parameters and are computationally complex, rendering them unsuitable for real-time blood pressure estimation.

IV. THE IMPACT OF INDIVIDUAL VARIATIONS ON THE ACCURACY OF BLOOD PRESSURE ESTIMATION

The BP is a quantification of the sideforce exerted by the circulating blood on the endothelial linings of blood vessels. Specifically, ABP

TABLE VI. Summary of the methods for estimating blood pressure from single PPG.

Study	Dataset	Algorithm	Result (mmHg)	
			SBP	DBP
75	Queensland 32 subjects	RT	ME: −0.1 SD: 6.5	ME: −0.6 SD: 5.2
76	MIMIC 44 subjects Queensland 31 subjects Guilin People's Hospital 219 subjects	RF, AdaBoost, XgBoost, LightGBM, CatBoost	MAE: 5.38 SD: 9.66	MAE: 3.05 SD: 4.88
77	Volunteers' data 205 subjects	Lasso Regression model	MAE:6.9 STD:9.0	MAE:5.0 STD:6.1
78	Volunteers' data 10 subjects	ARX models with kernel-based regularization	MEAN RMSE:6.5	
79	Volunteers' data 26 subjects	CNN	MAE:5.28	MAE:4.92
80	Volunteers' data 18 subjects	GA-LeNet/U-Net	MAE: 2.54	MAE: 1.48
81	Mindray dataset 467 subjects MIMIC	KD-Informer (transfer learning)	ME: 0.02 SD: 5.93	ME: 0.01 SD: 3.87
82	MIMIC III	CNN (superlet transform)	MAE: 2.71 SDAE: 3.29	MAE: 2.42 SDAE: 3.94
		Feat2Lab: LightGBM, SVR, RF, MLP, AdaBoost	Feat2Lab: SVR and LightGBM perform the best.	
83	Sensors, UCI, BCG, PPGBP	Sig2Lab: ResNet, spectroResNet, MLPBP Sig2Sig: U-Net, PPGIABP, V-Net	Sig2Lab: ResNet is the best model. Sig2Sig: U-Net perform the best. Across categories: Sig2Lab and Sig2Sig methods perform the best	

refers to the lateral pressure exerted by blood on the arterial wall during its flow within an artery, playing a crucial physiological role in ensuring adequate circulation. ABP exhibits normal physiological fluctuations that include the following:

(1) The circadian rhythm of ABP
ABP exhibits a distinct circadian rhythm, with diurnal peaks and nocturnal troughs in most individuals. Therefore, achieving optimal hypertension control necessitates maintaining blood pressure within the ideal range both during the day and at night.
(2) Sports
The response of BP to exercise is characterized by an increase in SBP, DBP, and mean arterial pressures. However, the increase in SBP demonstrates a more significant impact.
(3) Age and Gender
Age and gender disparities in ABP exist. Generally, pediatric individuals have lower ABP than adults. As age advances, adults show an increase in both SBP and DBP; however, the increase in SBP is greater than that of DBP. Adult males tend to have slightly higher ABP than females; however, these gender differences diminish following menopause.

A. The influencing factors of ABP

To establish a specific ABP, the vascular system must first be adequately filled with blood. Then, ventricular contraction propels blood into the aorta, converting its work into two forms of energy: kinetic energy that drives blood flow and potential energy stored in the arterial wall as elastic potential energy and pressure energy (systolic pressure). However, injected blood cannot generate sufficient ABP without peripheral resistance and ventricular ejection. After ventricular ejection ceases, elastic retraction occurs in the aorta and large arteries, converting stored potential energy into both pressure energy (diastolic pressure) and kinetic energy to drive blood flow.

Hence, the influencing factors of blood pressure encompass various determinants that impact the establishment of ABP, including circulating blood volume, stroke volume, peripheral resistance, elasticity of aortic, and large arterial wall, as well as heart rate.[84] Heart rate is calculated based on the time duration between R peaks identified in ECG recordings. In terms of aortic and large artery wall elastic properties, PTT can serve as a relevant characteristic parameter due to its close association with PWV. According to Lin *et al.*'s study,[85] selecting significantly correlated parameters serves as indicators of peripheral resistance and stroke volume. It is widely acknowledged from a medical perspective that the circulating blood volume corresponds to approximately 7%–8% of an individual's body weight. Weight can be considered a viable parameter for assessing circulating blood volume.

1. Stroke volume

Stroke volume pertains to the quantity of blood expelled into the aorta in one instance of contraction by the left cardiac ventricle. A rise

in the volume of blood pumped per heartbeat causes a greater flow of blood into the artery, leading to higher SBP, subsequently followed by DBP and pulse pressure (PP). Notably, SBP predominantly reflects the magnitude of stroke volume.

2. Heart rate

An increase in the heart rate results in a shortened ventricular diastole, reduced peripheral blood flow, and increased blood volume in the large arteries. This leads to an elevation of DBP and accelerated blood flow velocity, which in turn causes an increase in SBP. However, the rise in SBP is not as significant as that of DBP, resulting in a decrease in PP.

3. Peripheral resistance

Peripheral resistance is primarily generated in arterioles. An increase in peripheral resistance results in a significant reduction in blood flow velocity during diastole toward the heart's periphery. At the end of diastole, blood accumulates within the aorta, resulting in an elevation of both DBP and SBP; however, DBP increases more significantly than SBP, leading to a decrease in PP. Therefore, DBP mainly reflects the degree of peripheral resistance.

4. Elasticity of aorta and large artery wall

The significant rise in SBP, accompanied by a decline in DBP and a substantial increase in PP, can be attributed to the reduced elastic properties of the aorta and large artery walls. The effect of reduced elasticity on PP is particularly noticeable.

5. Circulating blood volume

The simultaneous decrease in both SBP and DBP is attributed to a reduction in circulating blood volume, with SBP demonstrating a more pronounced decline, thereby resulting in a decrease in PP.

All of the analyses mentioned assume that other variables remain constant and only consider the impact of a single factor on ABP. However, in practical scenarios, these five factors may change simultaneously, requiring a comprehensive consideration of all variables when analyzing factors that influence alterations in ABP.

B. The influence of circadian rhythm on BP

BP exhibits a circadian rhythm, with a decline during sleep and a gradual increase upon awakening.[86] In 1988, O'Brien *et al.*[87] reported that individuals with a mean diurnal BP difference of less than 10 or 5 mm Hg had a history of recurrent stroke; these individuals are referred to as non-dippers.[87] Normally, blood pressure decreases by approximately 10%–20% during the night compared to daytime levels, which defines the dipper pattern. However, individuals who exhibit less than a 10% decrease in nighttime blood pressure relative to daytime levels are classified as non-dippers, as shown in Table VII. Moreover, a nocturnal blood pressure drop of at least 20% is termed an extreme dipper. Conversely, if nighttime blood pressure exceeds daytime values (a ratio of nighttime to daytime blood pressure ≥ 1), it is referred to as a reverse-dipper, also known as an inverted dipper or rising type. Studies have shown that non-dipper and reverse-dipper individuals are more susceptible to severe target organ damage and exhibit higher cardiovascular risk compared to dippers.[88,89] Reverse-dipper individuals face significantly elevated risks (48%) for cardiovascular disease compared with dipper individuals,[90] particularly heart failure, which carries the greatest risk. Assessing nocturnal blood pressures is crucial as they hold greater relevance for mortality outcomes than daytime measurements.[88] Consequently, ABPM has become an essential method in the prevention and treatment of hypertension due to its capability to provide comprehensive data on diurnal and nocturnal blood pressure, as well as circadian rhythm patterns.

TABLE VII. Categorization of nocturnal blood pressure dipping in relation to daytime levels.

Reverse-dipper	Non-dipper	Dipper	Extreme dipper
$\geq 0\%$	$<0\%$–$<10\%$	$\leq 10\%$–$<20\%$	$\leq 20\%$

The discontinuous nature of current ABPM disrupts sleep. To tackle this issue, Radha *et al.*[91] employed wrist-worn PPG sensors and LSTM neural networks to devise a methodology for estimating nocturnal reductions in SBP based on the overall trends of BP during daily activities. The performance of LSTM was compared with traditional ML and non-ML approaches. The study found that the LSTM neural network was more effective, with a RMSE of 3.12 ± 2.20 mm Hg for the decrease in nocturnal SBP and a correlation coefficient of 0.69 with actual SBP decline. However, all estimation models used in the study had suboptimal accuracy and did not meet the requirements for practical application. To mitigate the impact of ABPM on sleep, work, and daily activities, Finnegan *et al.*[92] conducted a study on the correlation between PPG features and nocturnal BP patterns. The study selected PPG signals from 742 patients who were about to be discharged from the ICU from the MIMIC-III database and extracted 19 features to assess the correlation between their circadian rhythm and SBP circadian rhythm. The study found that five features had stronger correlations than HR. Additionally, combining these 19 PPG and PAT features significantly improved the accuracy of nighttime BP classification. However, it is necessary to note that this study was conducted at a population level rather than an individual level and did not include subjects who had been discharged from the hospital.

Therefore, exploring the construction of BP estimation models in diverse physiological states and forming model clusters for accurate BP estimation is worthwhile. Categorizing long-term BP data based on the circadian rhythm of human BP and developing specific models for different physiological states can effectively capture fluctuations caused by varying physiological conditions. During BP estimation, an adaptive selection process is used to choose the appropriate model from the cluster based on input characteristic parameters representing the individual's physiological state. This ensures self-calibration of the model.

V. DISCUSSION AND FUTURE RESEARCH DIRECTION

A. Discussion

This paper comprehensively elucidates the influence of PPG signal quality on blood pressure estimation. The subsequent analysis tasks heavily rely on denoising PPG signals and processing low-quality ones, which pose a significant challenge. Current methods relying on PPG waveform features and template matching exhibit limited accuracy and are prone to overfitting when applied to certain databases. Although ML/DL methods have demonstrated good performance in

quality assessment, they are limited by excessive model parameters, long computation time, and the requirement for a large amount of annotated data. These limitations prevent them from meeting the requirements of continuous signal quality assessment. Additionally, there is currently no standardized approach for handling missing signals or breakpoints caused by acquisition limitations or network transmission issues in practical scenarios. Typically, the nearest good PPG signal before and after the gap is used for interpolation of missing segments. Additionally, PPG signals exhibit variations in shape and amplitude across different body parts (fingers, wrists, upper arms, ears, etc.), detection methods (reflection or transmission), and subjects (age, gender, skin color, BMI, etc.). Furthermore, the current research lacks objective standards for evaluating signal quality and relies on subjective criteria. Therefore, it is imperative to establish unified evaluation standards and publicly available datasets with quality labels to validate assessment methods. Regrettably, no prior research has addressed this issue. To meet the real-time signal quality assessment requirements of portable devices while ensuring accuracy in assessment results, a lightweight model based on physiological principles should be employed for reconstructing clean PPG signals or more precise thresholds should be utilized to eliminate poor-quality signals.

Subsequently, the present article provides a comprehensive analysis of PPG signal-based methodologies for noninvasive BP estimation without the need for cuffs. The use of PWV or PTT for BP estimation requires at least two sensors, resulting in increased hardware cost and noise levels, making them non-portable. Additionally, these methods exhibit low estimation accuracy and require frequent calibration due to substantial physiological variability among individuals. Blood pressure estimation methods based on PWA exhibit significant result variations due to the extraction of numerous feature parameters and the complexity associated with screening methods for determining such parameters. Additionally, this approach may incorporate irrelevant features and fail to fully exploit information contained within the PPG waveform. Therefore, its effectiveness heavily relies on accurate detection of reference points within the waveform. Most ML techniques used for single PPG-based blood pressure estimation are only suitable for short-term measurements, failing to meet the requirements for long-term continuous beat blood pressure monitoring. Although attempts have been made to employ DL methodologies, their algorithmic black box nature poses challenges in terms of interpretability of feature parameters and estimation models within medical applications. Furthermore, DL models frequently require a large number of parameters and lengthy computation times, making them unsuitable for real-time BP estimation. Although many studies have investigated noninvasive continuous BP monitoring using PPG signals, current measurement methods and devices are limited to laboratory settings due to accuracy limitations, lack of portability, and frequent calibration requirements. Currently, the decrease in accuracy of continuous noninvasive cuffless blood pressure monitoring over extended durations and the frequent need for calibration can be attributed to several factors. First, noise interference on PPG signals, particularly motion artifacts, poses a significant challenge. This necessitates optimizing sensor design, employing robust sensing techniques, and enhancing signal quality. Additionally, more effective methods for assessing signal quality should be utilized to eliminate unusable signals. Second, it is necessary to identify features from PPG that are strongly correlated with BP. Currently, it is known that the correlation between PTT/PWV and BP is derived from the correlation between arterial compliance and pressure. However, whether there are other blood pressure-related features in the PPG waveform needs to be further investigated by researchers. Finally, the current BP estimation model has limitations as it only considers certain PPG and derived waveform features without fully incorporating physiological mechanisms and individual differences into its construction, consequently leading to low long-term estimation accuracy.

This article provides an overview of the factors that influence BP and highlights the impact of circadian rhythm on BP regulation. The factors include circulating blood volume, stroke volume, peripheral resistance, aortic and large artery wall elasticity, and heart rate. High-quality and uninterrupted monitoring of nocturnal BP is paramount due to the significant influence of circadian rhythm on blood pressure regulation, particularly during nocturnal hours when abnormal fluctuations pose serious health risks. However, research in this area remains insufficient. The incorporation of individual differences resulting from factors influencing BP and circadian rhythms should be taken into full consideration when developing BP estimation models, as individual differences may contribute to a decline in the accuracy of such models over time.

B. Future research direction

The dataset used in the current study has limitations in terms of demographic characteristics and quality criteria. To enhance the model's applicability and generalization ability, future research should aim to establish a more comprehensive and diverse dataset that incorporates annotated PPG signal quality. This will also provide a superior benchmark for comparison and evaluation purpose within the research field.

To address the urgent need for accurate and real-time evaluation of PPG signal quality, it is necessary to establish unified quality evaluation standards. Clean signals can be reconstructed from noisy signals using lightweight models based on physiology. Alternatively, more precise thresholds can be used to classify and remove poor PPG signals, while reasonable methods can be adopted to handle missing signals.

Currently, due to the lack of widely accepted PPG features that have strong connectivities with blood pressure, the identification of PPG features with clear physiological implications must be pursued in future studies. Additionally, it is important to deploy existing offline training models on mobile phones or other wearable devices, taking into account algorithmic accuracy, computational complexity constraints, and suitability for real-time blood pressure estimation. Consequently, developing lightweight and precise models presents a significant challenge for future research.

Previous studies have primarily focused on the average blood pressure level, which has low accuracy and requires frequent calibration. To account for inter-individual physiological differences and factors that influence blood pressure, future research should incorporate multiple physiological parameters and develop blood pressure estimation models based on circadian rhythms to form clusters of models. Accurate blood pressure estimation can be achieved by selecting appropriate models within these clusters based on changes in physiological characteristics.

Currently, commercialized wearable devices for CNIBP monitoring still face several challenges. These include inaccurate BP estimation, frequent calibration requirements, limited portability, and poor

comfort. To address these issues, it is important to optimize sensor design and utilize more robust sensing technologies to improve signal quality. Additionally, successful implementation of signal quality evaluation methods and continuous blood pressure estimation models, as mentioned in previous research directions, is necessary for further improvement. A comfortable wearing method is used to overcome interference caused by static water pressure changes and motion artifacts, and eliminate the need for cuff calibration based on a single PPG signal. These devices can effectively meet the accuracy requirements for long-term continuous ABPM.

Currently, the majority of self-generated datasets utilized in research are not publicly accessible, impeding the progress of research in this domain as other researchers have to replicate the process of generating their own datasets. We advocate for researchers to openly share their self-developed datasets and propose establishing a standardized framework for dataset composition, thereby facilitating better sharing and advancing progress in this field.

Furthermore, the current validation standards for blood pressure measurement devices primarily derive from the American Association for the Advancement of Medical Instrumentation (AAMI), the European Society of Hypertension (ESH), the Institute of Electrical and Electronics Engineers (IEEE), and the International Organization for Standardization (ISO). Almost all relevant studies adhere to these aforementioned standards for validation. However, it is worth noting that none of the first three standards propose specific validation criteria for continuous cuff-free blood pressure measurement. On the other hand, ISO 81060-3:2022 standardizes continuous noninvasive blood pressure validation by requiring each predicted blood pressure value to be outputted within a 30-s cycle and necessitating invasive arterial catheterization to obtain reference label values.[93] These requirements fail to meet ICU and operating room demands in terms of tracking rapid changes in blood pressure and are unsuitable for data collection outside these settings. Consequently, there is a need to develop new validation standards in future research on continuous noninvasive blood pressure that not only cater to tracking rapid fluctuations but also encompass diverse populations for data collection purpose. Additionally, there is a necessity to enhance the verification requirements for long-term stability of blood pressure accuracy, as well as validate the impact of different measurement positions relative to the heart level on blood pressure and assess the influence of physical movement on blood pressure. Henceforth, all forthcoming studies on continuous noninvasive blood pressure should undergo validation according to this novel standard.

VI. CONCLUSION

This article reviews the research progress of continuous monitoring technology for cuffless BP based on PPG. It covers the impact of PPG signal quality on BP estimation results, including PPG signal quality evaluation methods. It also discusses cuffless BP estimation technology based on PPG signals and the impact of individual differences on BP estimation accuracy, including factors affecting arterial blood pressure and the impact of circadian rhythm on BP. After analyzing and discussing the matter, it was determined that there are issues with the current process of CNIBP monitoring, from signal acquisition to BP estimation. Possible future research directions are suggested.

The completion of the proposed future research direction in this article could potentially reduce treatment costs for hypertensive patients worldwide and decrease the number of cardiovascular disease deaths caused by hypertension. Portable BP monitoring devices based on PPG and circadian rhythms can be utilized for continuous BP monitoring. Portable and comfortable wearable devices can be used to unconsciously and accurately track changes in BP throughout the day, including at night. This extensive review aims to contribute to the advancement of CNIBP measurement.

ACKNOWLEDGMENTS

This work was supported by the National Natural Science Foundation of China (Grant No. 81971700) and the Graduate Research Innovation Project in Chongqing, China (No. CYS23135).

AUTHOR DECLARATIONS

Conflict of Interest

The authors have no conflicts to disclose.

Ethics Approval

Ethics approval is not required.

Author Contributions

Gang Chen: Conceptualization (lead); Visualization (lead); Writing – original draft (lead). **Linglin Zou:** Project administration (lead); Writing – original draft (supporting). **Zhong Ji:** Conceptualization (lead); Funding acquisition (lead); Supervision (lead); Writing – review & editing (lead).

DATA AVAILABILITY

Data sharing is not applicable to this article as no new data were created or analyzed in this study.

REFERENCES

[1]World Health Organization, see https://www.who.int/news-room/fact-sheets/detail/hypertension for "Hypertension" (2023).
[2]A. Abiri, E.-F. Chou, C. Qian, J. Rinehart, and M. Khine, Sci. Rep. **12**(1), 16772 (2022).
[3]T. Greenhalgh, M. Knight, M. Inda-Kim, N. J. Fulop, J. Leach, and C. Vindrola-Padros, BMJ. **372**, n677 (2021).
[4]M. Cejnar, H. Kobler, and S. N. Hunyor, J. Biomed. Eng. **15**(2), 151–154 (1993).
[5]J. Allen, Physiol. Meas. **28**(3), R1–R39 (2007).
[6]M. Elgendi, Curr. Cardiol. Rev. **8**(1), 14–25 (2012).
[7]X. Xing and M. Sun, Biomed. Opt. Express **7**(8), 3007–3020 (2016).
[8]S. S. Mousavi, M. Firouzmand, M. Charmi, M. Hemmati, M. Moghadam, and Y. Ghorbani, Biomed. Signal Process. Control **47**, 196–206 (2019).
[9]J. Espina, T. Falck, J. Muehlsteff, Y. Jin, M. A. Adán, and X. Aubert, presented at the 2008 5th International Summer School and Symposium on Medical Devices and Biosensors, Hong Kong, China, 1–3 June 2008.
[10]L. Xu, D. Guo, F. E. H. Tay, and S. Xing, presented at the 2010 IEEE Conference on Sustainable Utilization and Development in Engineering and Technology, Kuala Lumpur, Malaysia, 20–21 November 2010.
[11]D. K. Jung, J. S. Ha, K. T. Kang, K. N. Kim, K. R. Kim, S. Y. Ye, J. H. Ro, and G. R. Jeon, J. Korean Soc. Med. Inf. **14**(3), 295–302 (2008).
[12]Y. A. Bhagat, K. Das, and T. Bui, presented at the Smart Biomedical and Physiological Sensor Technology XVIII, Online Only, 12–16 April 2021.
[13]Q. Zhang, D. Zhou, and X. Zeng, Biomed. Eng. Online **16**, 1–20 (2017).
[14]T. Wu, F. Wu, C. Qiu, J.-M. Redoute, and M. R. Yuce, IEEE Internet Things J. **7**(8), 6932–6945 (2020).

[15]E. S. Winokur, D. D. He, and C. G. Sodini, presented at the 2012 Annual International Conference of the IEEE Engineering in Medicine and Biology Society (EMBC), San Diego, CA, 28 August–1 September 2012.
[16]Y. Zheng, B. Leung, S. Sy, Y. Zhang, and C. C. Poon, presented at the 2012 Annual International Conference of the IEEE Engineering in Medicine and Biology Society (EMBC), San Diego, CA, 28 August–1 September 2012.
[17]J. Franco, J. Aedo, and F. Rivera, presented at the 2012 VI Andean Region International Conference, Cuenca, Ecuador, 7–9 November 2012 (2012).
[18]S. Puke, T. Suzuki, K. Nakayama, H. Tanaka, and S. Minami, presented at the 2013 35th Annual International Conference of the IEEE Engineering in Medicine and Biology Society (EMBC), Osaka, Japan, 3–7 July 2013.
[19]M. Atef, L. Xiyan, G. Wang, and Y. Lian, presented at the 2016 IEEE 59th International Midwest Symposium on Circuits and Systems (MWSCAS), Abu Dhabi, United Arab Emirates, 16–19 October 2016.
[20]W. S. W. Zaki, R. Correia, S. Korposh, B. R. Hayes-Gill, and S. P. Morgan, AIP Conf. Proc. **2203**, 020013 (2020).
[21]G. Bilo, C. Zorzi, J. E. O. Munera, C. Torlasco, V. Giuli, and G. Parati, Blood Pressure Monit. **20**(5), 291 (2015).
[22]G. Zhang, S. A. McCombie, R. Greenstein, and D. B. McCombie, presented at the 2014 36th Annual International Conference of the IEEE Engineering in Medicine and Biology Society (EMBC), Chicago, IL, 26–30 August 2014.
[23]Y. Li, Z. H. Lv, S. Y. Hu, Y. Q. Liu, J. B. Yan, H. Zhang, H. B. Li, Q. Chen, Y. Y. Li, Y.-F. Jiang, H. Zhou, M. D. Li, R. D. Chen, X. L. Li, S. S. Zhou, and Y. D. Chen, J. Geriatr. Cardiol. **19**(11), 843–852 (2022).
[24]L. Liu, Y. Wang, Y. Li, X. Feng, H. Song, Z. He, and C. Guo, Circuits, Syst., Signal Process. **38**(9), 4096–4114 (2019).
[25]Pankaj, A. Kumar, M. Kumar, and R. Komaragiri, IEEE Trans. Instrum. Meas. **71**, 4006910 (2022).
[26]X. Ma, D. Zhang, and Y. Zhang, J. Eng. **2020**(11), 1088–1094.
[27]E. Bou Assi, D. K. Nguyen, S. Rihana, and M. Sawan, Biomed. Signal Process. Control **34**, 144–157 (2017).
[28]G. Bortolan, I. Christov, I. Simova, and I. Dotsinsky, Biomed. Signal Process. Control **18**, 378–385 (2015).
[29]S. Nagai, D. Anzai, and J. Wang, Healthcare Technol. Lett. **4**(4), 138–141 (2017).
[30]J. Lee, M. Kim, H.-K. Park, and I. Y. Kim, Sensors **20**(5), 1493 (2020).
[31]D. Pollreisz and N. TaheriNejad, Mobile Networks Appl. **27**(2), 728–738 (2019).
[32]D. Seok, S. Lee, M. Kim, J. Cho, and C. Kim, Front. Electron. **2**, 685513 (2021).
[33]K. J. Reynolds, J. P. Dekock, L. Tarassenko, and J. T. B. Moyle, Br. J. Anaesth. **67**(5), 638–643 (1991).
[34]J. N. Adler, L. A. Hughes, R. Vivilecchia, and C. A. Camargo, Acad. Emerg. Med. **5**(10), 965–970 (1998).
[35]X. F. Teng and Y. T. Zhang, Physiol. Meas. **27**(8), 675–684 (2006).
[36]X.-Y. Zhang and Y.-T. Zhang, Physiol. Meas. **27**(7), 649–660 (2006).
[37]C. Lee, H. S. Shin, J. Park, and M. Lee, IEEE Sens. J. **12**(5), 1253–1254 (2012).
[38]T. Desquins, F. Bousefsaf, A. Pruski, and C. Maaoui, Appl. Sci. **12**(19), 9582 (2022).
[39]R. Donida Labati, V. Piuri, F. Rundo, and F. Scotti, Pattern Recognit. Lett. **156**, 119–125 (2022).
[40]E. Mejía-Mejía, J. Allen, K. Budidha, C. El-Hajj, P. A. Kyriacou, and P. H. Charlton, *Photoplethysmography* (Elsevier Ltd, 2022), pp. 69–146.
[41]M. Elgendi, Bioengineering **3**(4), 21 (2016).
[42]Y. B. Liang, M. Elgendi, Z. C. Chen, and R. Ward, Sci. Data **5**, 180076 (2018).
[43]K. Hayashi, Y. Maeda, T. Yoshimura, M. Huang, and T. Tamura, Sensors **23**(17), 7399 (2023).
[44]W.-H. Lin, N. Ji, L. Wang, and G. Li, presented at the 2019 41st Annual International Conference of the IEEE Engineering in Medicine and Biology Society (EMBC), Berlin, Germany, July 23–27 2019.
[45]T. Banerjee, R. D. Gavas, B. Mithun, S. Karmakar, R. K. Ramakrishnan, and A. Pal, presented at the 2022 44th Annual International Conference of the IEEE Engineering in Medicine & Biology Society (EMBC), Glasgow, Scotland, United Kingdom, 11–15 July 2022.
[46]M. S. Roy, R. Gupta, and K. D. Sharma, IEEE Trans. Instrum. Meas. **71**, 2519709 (2022).
[47]M. Salah, O. A. Omer, L. Hassan, M. Ragab, A. M. Hassan, and A. Abdelreheem, IEEE Access **10**, 55616–55626 (2022).
[48]P. Prasun, S. Mukhopadhyay, and R. Gupta, Meas. Sci. Technol. **33**(1), 015701 (2021).
[49]A. Adami, R. Boostani, F. Marzbanrad, and P. H. Charlton, IEEE Access **9**, 45832–45844 (2021).
[50]X. Fan and T. Tjahjadi, Pattern Recognit. Lett. **137**, 12–16 (2020).
[51]J. Schmith, C. Kelsch, B. C. Cunha, L. R. Prade, E. A. Martins, A. L. Keller, and R. M. D Figueiredo, Biomed. Signal Process. Control **86**, 105142 (2023).
[52]A. Tiwari, G. Gray, P. Bondi, A. Mahnam, and T. H. Falk, Sensors **23**(12), 5606 (2023).
[53]C. Orphanidou, in *Signal Quality Assessment in Physiological Monitoring: State of the Art and Practical Considerations* (Springer International Publishing, Cham, 2018), pp. 41–61.
[54]P. K. Lim, S.-C. Ng, N. H. Lovell, Y. P. Yu, M. P. Tan, D. McCombie, E. Lim, and S. J. Redmond, Physiol. Meas. **39**(10), 105005 (2018).
[55]G. B. Papini, P. Fonseca, L. M. Eerikäinen, S. Overeem, J. W. M. Bergmans, and R. Vullings, Physiol. Meas. **39**(11), 115007 (2018).
[56]J. Song, D. Li, X. Ma, G. Teng, and J. Wei, Biomed. Signal Process. Control **47**, 88–95 (2019).
[57]S. Alam, R. Gupta, and K. D. Sharma, IEEE Trans. Instrum. Meas. **70**, 1–9 (2021).
[58]H. Yang, M. Li, D. He, X. Che, and X. Qin, presented at the 2019 IEEE International Conference on Mechatronics and Automation (ICMA), Tianjin, China, 4–7 August 2019.
[59]A. H. Gazi, S. Sundararaj, A. B. Harrison, N. Z. Gurel, M. T. Wittbrodt, M. Alkhalaf, M. Soudan, O. Levantsevych, A. Haffar, and A. J. Shah, presented at the 2021 43rd Annual International Conference of the IEEE Engineering in Medicine & Biology Society (EMBC), ELECTR NETWORK, 1–5 November 2021.
[60]S.-H. Liu, J.-J. Wang, W. Chen, K.-L. Pan, and C.-H. Su, Appl. Sci. **10**(4), 1476 (2020).
[61]D. Roh and H. Shin, Sensors **21**(6), 2188 (2021).
[62]M. Rinkevičius, P. H. Charlton, R. Bailón, and V. Marozas, Sensors **23**(4), 2220 (2023).
[63]Z. Chen, B. S. Dees, and D. P. Mandic, presented at the 2020 International Joint Conference on Neural Networks (IJCNN), Tianjin, China, 4–7 August 2020.
[64]A. I. Moens, in *Die pulscurve* (Brill, Leiden, The Netherlands, 1878).
[65]D. J. Korteweg, Annalen der Phys. **241**(12), 525–542 (1878).
[66]R. Lazazzera, Y. Belhaj, and G. Carrault, Sensors **19**(11), 2557 (2019).
[67]F. Tabei, J. M. Gresham, B. Askarian, K. Jung, and J. W. Chong, IEEE Access **8**, 11534–11545 (2020).
[68]D. Marzorati, D. Bovio, C. Salito, L. Mainardi, and P. Cerveri, IEEE Access **8**, 55424–55437 (2020).
[69]T. H. Huynh, R. Jafari, and W.-Y. Chung, IEEE Trans. Biomed. Eng. **66**(4), 967–976 (2019).
[70]P. Yousefian, S. Shin, A. Mousavi, C.-S. Kim, R. Mukkamala, D.-G. Jang, B.-H. Ko, J. Lee, U. K. Kwon, Y. H. Kim, and J.-O. Hahn, Sci. Rep. **9**(1), 10666 (2019).
[71]S. Chen, Z. Ji, H. Wu, and Y. Xu, Sensors **19**(11), 2585 (2019).
[72]X. Tan, Z. Ji, Y. Zhang, C. Gómez, S. P. Schwarzacher, and H. Zhou, Technol. Health Care **26**, 87–101 (2018).
[73]Y.-H. Li, L. N. Harfiya, K. Purwandari, and Y.-D. Lin, Sensors **20**(19), 5606 (2020).
[74]U. Senturk, K. Polat, and I. Yucedag, Appl. Acoust. **170**, 107534 (2020).
[75]S. G. Khalid, J. Zhang, F. Chen, and D. Zheng, J. Healthcare Eng. **2018**, 1–13.
[76]Q. Hu, X. Deng, A. Wang, and C. Yang, Physiol. Meas. **41**(12), 125009 (2020).
[77]J. Dey, A. Gaurav, and V. N. Tiwari, presented at the 2018 40th Annual International Conference of the IEEE Engineering in Medicine and Biology Society (EMBC), Honolulu, Hawaii, USA, 18–21 July 2018.
[78]G. Acciaroli, A. Facchinetti, G. Pillonetto, and G. Sparacino, presented at the 2018 40th Annual International Conference of the IEEE Engineering in Medicine and Biology Society (EMBC), Honolulu, Hawaii, USA, 18–21 July 2018.
[79]S. Baek, J. Jang, S.-H. Cho, J. M. Choi, and S. Yoon, presented at the 2020 42nd Annual International Conference of the IEEE Engineering in Medicine & Biology Society (EMBC), Montreal, Quebec, Canada, 20–24 July 2020.

[80]M. Sadrawi, Y.-T. Lin, C.-H. Lin, B. Mathunjwa, S.-Z. Fan, M. F. Abbod, and J.-S. Shieh, Sensors **20**(14), 3829 (2020).
[81]C. Ma, P. Zhang, F. Song, Y. Sun, G. Fan, T. Zhang, Y. Feng, and G. Zhang, IEEE J. Biomed. Health Inf. **27**(5), 2219–2230 (2023).
[82]Pankaj, A. Kumar, R. Komaragiri, and M. J. P. Kumar, Phys. Eng. Sci. Med. **46**(4), 1589–1605 (2023).
[83]S. González, W.-T. Hsieh, and T. P.-C. Chen, Sci. Data **10**(1), 149 (2023).
[84]K. Sembulingam and P. Sembulingam, in *Essentials of Medical Physiology* (JP Medical Ltd, 2012), pp. 519–672.
[85]W.-H. Lin, X. Li, Y. Li, G. Li, and F. Chen, Physiol. Meas. **41**(4), 044003 (2020).
[86]Y. Cheng, Y. Li, and J. Wang, Chin. Med. J. **135**(9), 1027–1035 (2022).
[87]E. O'Brien, J. Sheridan, and K. O'Malley, Lancet **2**(8607), 397 (1988).
[88]J. Boggia, Y. Li, L. Thijs, T. W. Hansen, M. Kikuya, K. Björklund-Bodegård, T. Richart, T. Ohkubo, T. Kuznetsova, C. Torp-Pedersen, L. Lind, H. Ibsen, Y. Imai, J. Wang, E. Sandoya, E. O'Brien, and J. A. Staessen, Lancet **370**(9594), 1219–1229 (2007).
[89]W.-Y. Yang, J. D. Melgarejo, L. Thijs, Z.-Y. Zhang, J. Boggia, F.-F. Wei, T. W. Hansen, K. Asayama, T. Ohkubo, J. Jeppesen, E. Dolan, K. Stolarz-Skrzypek, S. Malyutina, E. Casiglia, L. Lind, J. Filipovský, G. E. Maestre, Y. Li, J.-G. Wang, Y. Imai, K. Kawecka-Jaszcz, E. Sandoya, K. Narkiewicz, E. O'Brien, P. Verhamme, and J. A. Staessen, Jama **322**(5), 409 (2019).
[90]K. Kario, S. Hoshide, H. Mizuno, T. Kabutoya, M. Nishizawa, T. Yoshida, H. Abe, T. Katsuya, Y. Fujita, O. Okazaki, Y. Yano, N. Tomitani, and H. Kanegae, Circulation **142**(19), 1810–1820 (2020).
[91]M. Radha, K. de Groot, N. Rajani, C. C. P. Wong, N. Kobold, V. Vos, P. Fonseca, N. Mastellos, P. A. Wark, N. Velthoven, R. Haakma, and R. M. Aarts, Physiol. Meas. **40**(2), 025006 (2019).
[92]E. Finnegan, S. Davidson, M. Harford, J. Jorge, M. Villarroel, and L. Tarassenko, presented at the 2022 44th Annual International Conference of the IEEE Engineering in Medicine & Biology Society (EMBC), Glasgow, Scotland, United Kingdom, 11–15 July 2022.
[93]International Organization for Standardization, see https://www.iso.org/standard/ISO for "ISO: Global standards for trusted goods and services" (2022).